Integrated high voltage power supply utilizing burst mode control and its performance impact on dielectric electro active polymer actuators

T. Andersen*, M.S. Rødgaard*, M.A.E. Andersen*, O.C. Thomsen*, K. P. Lorenzen†, C. Mangeot‡, A. R. Steenstrup‡
*Technical University of Denmark, DTU Elektro, Kgs. Lyngby, Denmark
†Danfoss PolyPower A/S, Nordborg, Denmark
‡Noliac A/S, Noliac Motion, Kvistgaard, Denmark

Abstract:
Through resent years new high performing Dielectric Electro Active Polymers (DEAP) have emerged. To fully utilize the potential of DEAPs a driver with high voltage output is needed. In this paper a piezoelectric transformer based power supply for driving DEAP actuators is developed, utilizing a burst mode control technique. Controlling and driving a DEAP actuator between 250V to 2.5kV is demonstrated, where discrete like voltage change and voltage ripple is observed, which is introduced by the burst mode control. Measurements of the actuator strain-force reveal that the voltage ripples translates to small strain-force ripples. Nevertheless the driver demonstrates good capabilities of following an input reference signal, as well as having the size to fit inside a 110 mm x 32 mm cylindrical InLastor Push actuator, forming a "low voltage" DEAP actuator.

Keywords: Dielectric Electro Active Polymers, Driver, Power supply, Piezoelectric transformer

Introduction

The resent years emergence of new high performing DEAP materials, calls for higher performing drivers in order to fully utilize its potential. Figure 1 top illustrates the state of the art driver for driving the cylindrical InLastor Push actuator. The driver is electromagnetic transformer (EMT) based and converts the input DC voltage of 24 volt to an output voltage between 250V and 2.5kV depending on a control signal.
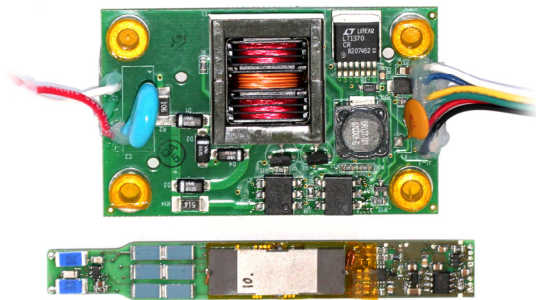

Figure 1: *Converters for driven DEAP actuators. Top: The state of the art electromagnetic (EMT) based driver. Bottom: Novel piezoelectric transformer (PT) based driver*

At the bottom of figure 1 the novel piezoelectric transformer (PT) based driver is illustrated. It utilizes an inductor less topology which enables operation in high external magnetic fields, as well as the elimination of bulky inductors reduces overall volume. The decrease in volume of the PT based driver allows the driver to be integrated into a cylindrical DEAP actuator, which is illustrated in

figure 2. The benefits of integrating the driver into the DEAP are to avoid the high voltage interface. Issues regarding high voltage safety are avoided. The availability of low voltage power supplies is far greater than for high voltage.
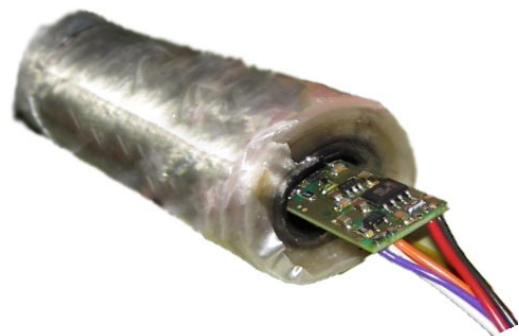

Figure 2: *Cylindrical DEAP actuator with integrated driver. The driver is pulled a bit out of the actuator for the purpose of illustration*

In this work the performance of the novel PT based driver is compared with the state of the art EMT based driver. The general design will be presented, as well as the basic operation and functionality. The efficiency and EMI performance will be compared and evaluated. Furthermore the performance of the resulting integrated cylindrical DEAP actuator is presented and evaluated.

Inductor-less PT based driver

The principle of an inductor-less PT based driver relies on a half-bridge driven PT topology [1]. The electrical equivalent of a PT, valid in the vicinity of a single resonance mode, can be modeled with the Mason lump parameter equivalent [2-4]. The Mason equivalent connected with a half-bridge is illustrated in figure 3. The capacitance C_{d1} is large, easily 100 times greater than the output capacitance of the two MOSFETs. The high capacity load on the half-bridge is a disadvantage. Each time the half-bridge voltage (V_1) is hard switched the stored energy in C_{d1} is dissipated in the MOSFETs.
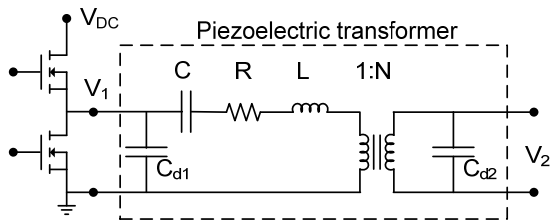

Figure 3: *Inductor-less PT topology. Half-bridge connected with the Mason equivalent model of a piezoelectric transformer*

To improve efficiency of the converter the half-bridge must be soft switched instead of hard switched. Soft switching is in this case referred to as zero voltage switching (ZVS) and occurs when the voltage across the MOSFET is zero when it turns on. ZVS can be obtained by the PT, however the PT and the control must be optimized for ZVS operation [1, 5-7].

The driver utilizes an interleaved multilayer Rosen type transformer [8], which is ZVS optimized. Figure 4 sketches the structure of the PT and the polarization directions and for simplification only two primary layers are shown.
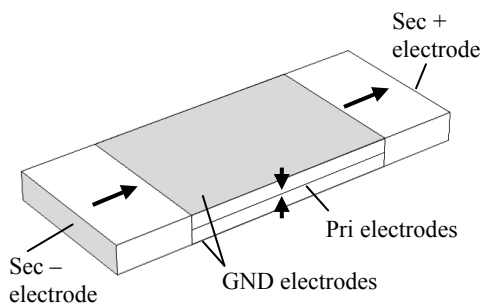

Figure 4: *The interleaved multi layer Rosen-type PT structure, where the arrows indicate the polarization direction. Size: 30mm x 10mm x 2mm*

The secondary sections of the transformer are polarized in the same direction. Thereby the output voltage of the two secondary electrodes is 180 degrees out of phase, which increase the gain of the transformer. The equivalent model of the PT is illustrated in figure 5. To further increase the overall step-up ratio of the converter a voltage doubler rectifier circuit is utilized at the output of the PT [9, 10]. However a three diode version is used instead of the standard two diode solution. This is necessary for the ground referred output voltage feedback circuit to work correctly, as well as avoiding a large common mode voltage signal over the actuator.
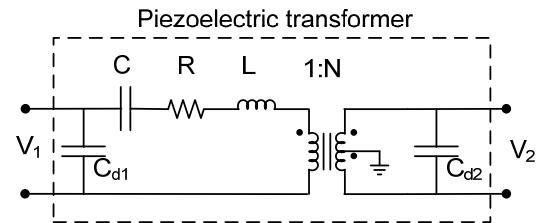

Figure 5: *Electrical equivalent of the interleaved Rosen type transformer, with both secondary sections polarized in the same direction*

To ensure high efficiency of the converter a inner closed-loop control circuit similar to [11] is used to maintain ZVS operation of the PT. An outer closed-loop is controlling the output voltage in a bust mode (quantum-mode) manner [11-13]. Feedback from the output voltage across the DEAP actuator closes the outer loop. Decrease of the output voltage is done by discharging the DEAP actuator through a resistive network. Figure 6 illustrates the driver with the DEAP connected.
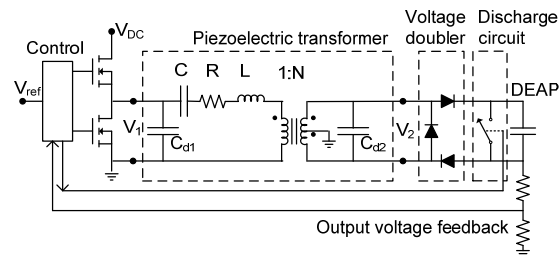

Figure 6: *Block diagram of inductor-less PT converter with voltage doubler rectifier, discharging circuit and DEAP actuator connected*

A reference signal (V_{ref}) is controlling the voltage across the DEAP actuator. When the output voltage feedback is below the reference signal the driver is turned on. When the output voltage feedback is above the reference signal the driver is turned off and the discharging circuit is turned on.
With a constant reference signal, the driver will charge the DEAP to the output voltage corresponding to the reference signal and then turn off the driver. The DEAP will retain the output voltage, however leakage current within the DEAP and the diodes together with the current drawn by

the output voltage feedback circuit is slowly discharging the DEAP. When the DEAP is discharge below a certain lower threshold of the reference signal, the driver is turned on again to charge the DEAP until a certain upper threshold of the reference signal. This control method is referred to as burst mode control. Figure 7 shows an oscilloscope plot of the PT driver in action. Notice that the voltage of the DEAP is attenuated by 1000 times. The time between each burst is determined by the discharge rate of the DEAP and the hysteretic window around the reference signal. The time length of each burst is controlled by adjusting the hysteretic window around the reference signal. The size of the hysteretic window is a trade-off between efficiency and output voltage ripple. As the hysteretic window goes towards zero the burst frequency and burst time length goes towards zero, decreasing the output voltage ripple. However efficiency will drop as the time length of each burst decreases. The explanation is that it takes time to build up the necessary resonance current within the PT for ZVS operation. Every start-up of the PT is therefore very inefficient compared to ZVS operation.
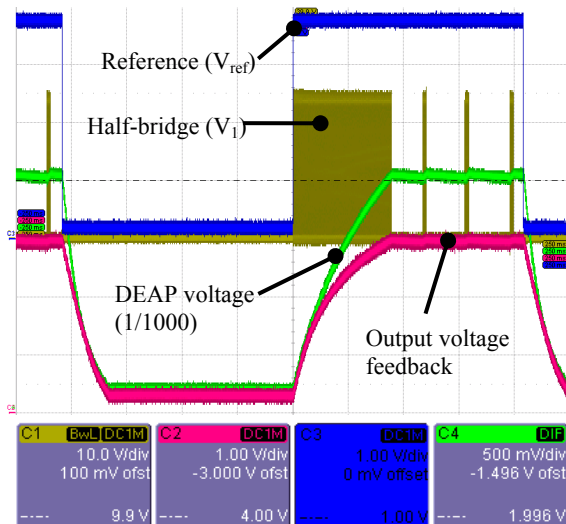

Figure 7: *Oscilloscope plot of the PT based driver with a square wave reference signal. Burst mode control of the half-bridge is observed. DEAP voltage is attenuated by x1000*

Driver performance

In this section the electrical properties of the PT based driver is compared to the state of the art EMT based driver.

Efficiency
The efficiency of the driver is defined as the ratio between energy stored in the DEAP and energy delivered to the driver (1). Figure 8 shows the used setup for measure the efficiency of the two drivers. Prior to the measurement output is discharged to zero volt. The input voltage is 24 volt and the

DEAP is substituted with a fixed capacitance of 47nF. The input current is measured as the output capacity is charged from zero to 1.9kV.

$$\eta = \frac{E_{DEAP}}{E_{input}} = \frac{0.5 \cdot C_{DEAP} \cdot V_{DEAP}^2}{\int V_{DC} \cdot I_{in} \cdot dt} \quad (1)$$
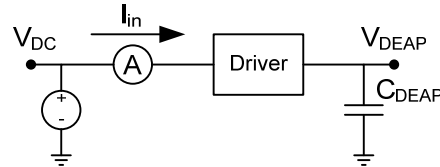

Figure 8: *Setup for measure efficiency of the driver*

The measured input current for the PT based and EMT based driver is plotted in figure 9. When the output voltage reached 1.9kV the control circuit turns off the half-bridge stage and the input current drops sudden and only auxiliary current consumption is left.
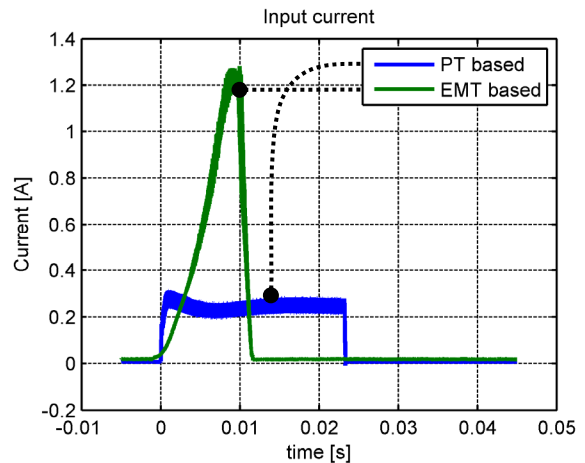

Figure 9: *Measurement of input current while charging the output voltage from 0V to 1.9kV*

From the measured input current and the definition (1) is the efficiency calculated for both drivers, see table 1.

Driver type:	E_{input} (24V)	E_{DEAP} (47nF)	Efficiency
PT based	138mJ	81.2mJ	58.8%
EMT based	182mJ	82.4mJ	45.3%

Table 1: *Efficiency of PT based and EMT based driver*

$$PT_{loss\,reduction} = \frac{E_{loss,EMT} - E_{loss,PT}}{E_{loss,EMT}} = 41\% \quad (2)$$

The energy loss for PT based driver is reduced by 41% compared to the EMT based driver (2).
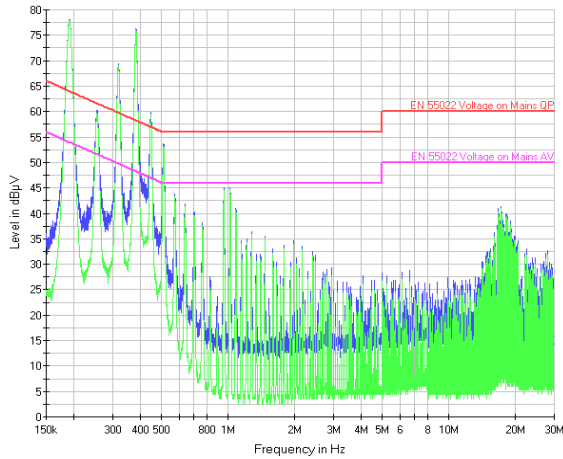
Figure 10: *EMI measurement of PT based driver at 4 watts output power*

EMI
As the PT based driver does not contain any magnetic components, the emitted magnetic fields are expected to be low. But this also means that the driver has no input filter to suppress the fundamental switching frequency. As the PT based driver is a soft switched resonance converter, the general EMI performance is expected to be good.

The setup used for the measurement the conducted EMI is illustrated in figure 11. The LISN network is connected to an EMC receiver. The utilized EMC receiver requires a steady state operation of the device under test in order to measure the EMI correct. The driver is therefore loaded with a resistive load (R_L) instead of a capacitive load.
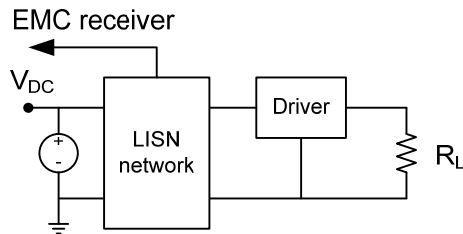

Figure 11: *Setup for measure conducted EMI*

The result of the EMC receiver is shown in figure 10 and figure 12 for the PT based and the EMT based driver respectively. Both measurements are performed with an output power of 4 watts. None of the drivers have any dedicated EMI filtering. As expected both drivers lacks the ability to suppress fundamental frequencies with a peak of around 80dBµV. However the PT based driver performs well in the high frequency region (above 1MHz) with a ≈25dBµV decrease between the peak values compared with the EMT based driver.
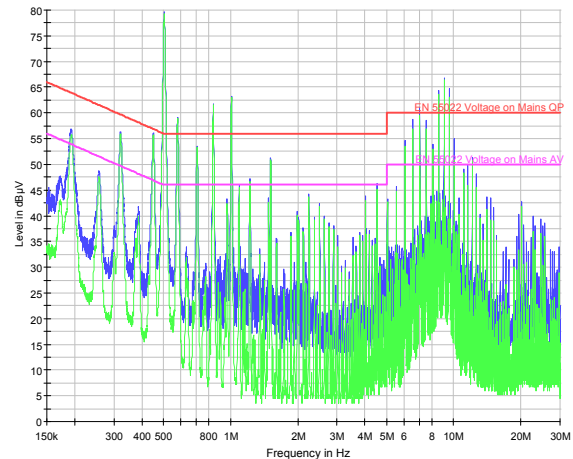

Figure 12: *EMI measurement of EMT based driver at 4 watts output power*

DEAP performance with integrated driver

The mechanical performance of the integrated DEAP actuator is evaluated trough a Stroke-Force measurement. The measurement is performed by prevent the movement of the actuator, when applying the voltage. The actuator is then slowly released, while the force and stroke is measured. Stroke-Force measurements of the DEAP actuator, with and without driver integration, are shown in figure 13.
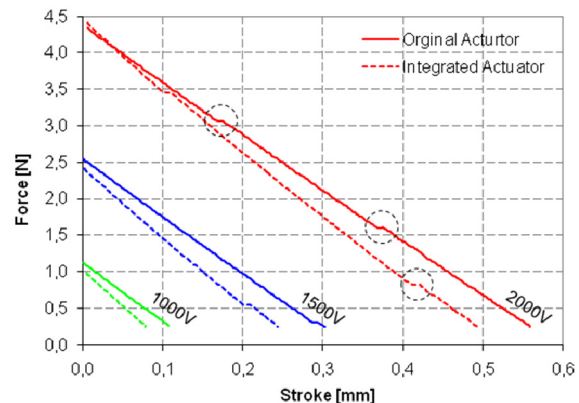

Figure 13: *Stroke-Force measurement of the DEAP actuator, with and without driver integration, at different DEAP voltages*

It can be seen that the integration do decrease the stroke performance somewhat. Approximately 12% decrease in stroke. This is due to increased tension and friction, as the PCB is attached in one end of the actuator and is sliding in a slot in the other end. Furthermore small jumps can be observed on the measurements. This is small burst from the driver, as the voltage drops due to the increase in capacitance, as the film is getting thinner. The driver will counteract this drop as it will maintain a constant output voltage.

Conclusion

The basic structure and operational functionality of the novel PT based DEAP actuator driver are presented in this work. Furthermore the performance is compared with the state of the art EMT based driver, as well as the performance of the resulting integrated DEAP actuator is evaluated. The PT based driver demonstrated a 14% point increase in efficiency, compared to the EMT based driver, resulting in a 41% loss reduction. The EMI performance of the PT based driver showed a good improvement of 25dBμV in the high frequency region (above 1MHz). Finally the resulting integrated cylindrical DEAP actuator demonstrated full functionality, with approximately 12% decrease in stroke performance, compared to the original actuator.

References

[1] J. M. Alonso, C. Ordiz, and M. A. Dalla Costa, "A novel control method for piezoelectric-transformer based power supplies assuring zero-voltage-switching operation," *Industrial Electronics, IEEE Transactions on,* vol. 55, pp. 1085-1089, 2008.

[2] C. Lin and F. Lee, "Design of a piezoelectric transformer converter and its matching networks," 1994, pp. 607-612 vol. 1, ISBN: 0780318595.

[3] G. Zerong, J. Lingling, L. Huabo, and W. Ting, "Measurement of PT equivalent circuit model parameters based on admittance circle," 2011, pp. 20-23, ISBN: 1612847196.

[4] C. Lin, "Design and analysis of piezoelectric transformer converters," PhD Dissertation, 1997.

[5] E. Horsley, N. Nguyen-Quang, M. Foster, and D. Stone, "Achieving ZVS in inductor-less half-bridge piezoelectric transformer based resonant converters," 2009, pp. 446-451, ISBN: 1424441668.

[6] S. Bronstein and S. Ben-Yaakov, "Design considerations for achieving ZVS in a half bridge inverter that drives a piezoelectric transformer with no series inductor," 2002, pp. 585-590 vol. 2, ISBN: 078037262X.

[7] K. S. Meyer, M. A. E. Andersen, and F. Jensen, "Parameterized analysis of Zero Voltage Switching in resonant converters for optimal electrode layout of Piezoelectric Transformers," 2008, pp. 2543-2548, ISBN: 1424416671.

[8] M. S. Rødgaard, T. Andersen, K. S. Meyer, and M. A. E. Andersen, "Design of interleaved multilayer rosen type piezoelectric transformer for high voltage DC/DC applications," in *PEMD*, 2012.

[9] G. Ivensky, M. Shvartsas, and S. Ben-Yaakov, "Analysis and modeling of a voltage doubler rectifier fed by a piezoelectric transformer," *Power Electronics, IEEE Transactions on,* vol. 19, pp. 542-549, 2004.

[10] G. Ivensky, S. Bronstein, and S. Ben-Yaakov, "A comparison of piezoelectric transformer AC/DC converters with current doubler and voltage doubler rectifiers," *Power Electronics, IEEE Transactions on,* vol. 19, pp. 1446-1453, 2004.

[11] J. Diaz, J. Martin-Ramos, M. Prieto, and F. Nuno, "A double-closed loop DC/DC converter based on a piezoelectric transformer," 2004, pp. 1423-1428 Vol. 3, ISBN: 0780382692.

[12] J. A. Martin-Ramos, M. A. J. Prieto, F. N. García, J. D. González, and F. M. F. Linera, "A new full-protected control mode to drive piezoelectric transformers in DC-DC converters," *Power Electronics, IEEE Transactions on,* vol. 17, pp. 1096-1103, 2002.

[13] J. Díaz, F. Nuño, J. M. Lopera, and J. A. Martín-Ramos, "A new control strategy for an AC/DC converter based on a piezoelectric transformer," *Industrial Electronics, IEEE Transactions on,* vol. 51, pp. 850-856, 2004.